A Preliminary Investigation of Open-Ended Evolution in Two-Dimensional Discrete Dynamical Systems

Perry W. Swanborough

Abstract

Open-ended evolution (OEE) of interacting elementary cellular automata (ECA) was studied by Alyssa Adams et al. (2017). Some instances of composite ECA systems incorporating state-dependent dynamics were shown to satisfy definitions of unbounded evolution (UE) and innovation (INN), facilitating OEE. As an exercise in the rigorous analysis of systems not larger than sufficient to establish universal requirements for OEE, the scope of the study was restricted to small one-dimensional systems (ECAs) in which the perturbation of one subsystem by one other was one-way only (from "environment", e to "organism", o), but the authors recognized that their conclusions should also be relevant to the richer dynamics of large systems of mutually interacting subsystems. In this study, I explore the potential of three mutually interacting hodge podge machines for OEE and recognize that study of OEE in such comparatively large systems is provisionally tractable only by assessment of INN, considered as a reliable UE/OEE indicator.

Keywords: Belousov-Zhabotinsky reaction, cellular automata, hodge podge machine, innovation, open-ended evolution, unbounded evolution

Introduction

Persistence of unpredictable change is an amazing feature of the world which we can describe as *open-ended evolution* (OEE). An unsolved deep problem is that attempts to model the evolution of the world and its processes have failed to capture OEE, but recognition that OEE incorporates *unbounded evolution* (UE) and *innovation* (INN) points the way to discernment of what is missing from dynamics models which fail to exhibit increasing diversification. The OEE problem has been studied with composite systems of elementary cellular automata (ECA) in which one subsystem perturbs the state trajectory of another, and determining if rigorous definitions of UE and INN are satisfied [1].

Understanding OEE requires definitions of its defining features. A system of finite size accommodating only a finite number of states must eventually cycle within an expected recurrence time: the *Poincaré recurrence time* (t_p). Note that many dynamical systems will never return to an initial state, but will enter a limit cycle spanning a small subset of all otherwise-possible states, often with a short period. A prospective subsystem evolving in isolation will cycle within its own t_p but recurrence of a subsystem (t_r) within a composite system of interacting subsystems can exceed the t_p of its isolated equivalent. The definition of UE follows: it corresponds to $t_r > t_p$ [1]. The other OEE feature, innovation (INN), is defined to have occurred if a subsystem's state trajectory is not a possible state trajectory of its isolated equivalent [1].

In [1], three categories of one-dimensional ECA systems incorporating one subsystem ("environment", e) perturbing another ("organism", o) were described. In two of them (case categories 2 and 3), the rule evolution of o is entirely driven by external influence: in case 2, the eight-bit state of an environment ECA is interpreted as the ECA rule applying to o at each time step, and in case 3, the state trajectory of o is determined by stochastic bit-flips of the ECA rule table applied at each iteration. The state-dependency exclusive to case category 1 system dynamics was inspired by recognition of the self-referential nature of biological dynamics: only in case 1 systems is

the state trajectory of o determined by both its own state and perturbations of its rule at each step by its environment.

Figure 1 below shows an example of a case 1 system demonstrating OEE, reproduced from [1].

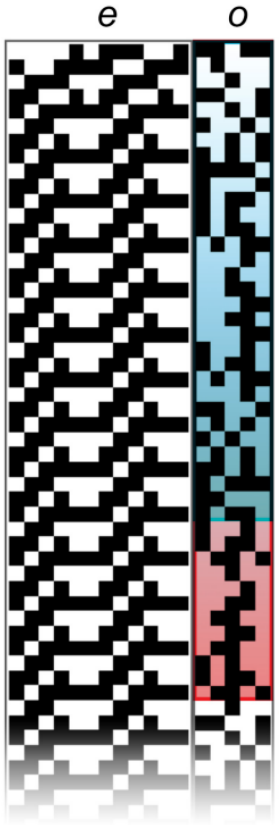

Figure 1. A case 1 system exhibiting OEE, reproduced from [1]. With black cells corresponding to state 1 and white cells representing state 0, the time trajectory of e (environment) is determined by repeated application of ECA rule 62: 00111110 (Wolfram's ECA indexing scheme, [6]). The first state (top row) of o (organism) is 11011 which transitions to 01000 by rule 66 (01000010). Subsequent evolution of the o state is determined by environmental modification of the transition rule at each step as specified in [1]. By the algorithm, the specific sequence of rules applied to o is 66 → 80 → 67 → 25 → 57 → 43 → 29 → 117 → 61 → …

In Figure 1 the organism o is five cells (bits) wide (2^5 = 32 possible states) so t_p = 32 steps, shown by blue highlight. The longer states recurrence time (t_r) is indicated by the red highlight extending further than the blue highlight. The 42-step state sequence from the third o state 00100 to the state where the red highlight ends (01101) repeats indefinitely, so t_r = 42 steps > t_p = 32 steps, meeting the definition of UE. The sequence of rules (t'_r) applying to o also repeats each 42 steps (but note $t_r = t'_r$ does not always occur in these systems).

By inspection of the 42-step t_r cycle, neighbourhood 111 always corresponds to cell state transition 1 to 0 but contradictions (state transitions to 0 **and** 1) occur from instances of all other three-cell neighbourhoods within the t_r cycle. Occurrence of such contradictions reveals innovation (INN), *i.e*.

the t_r sequence cannot be the outcome of any single ECA rule uniformly applied. The definitions of UE and INN are both met by the system of Figure 1, so it demonstrates OEE as defined in [1].

(As an aside, the perpetually-repeating 42-step t_r sequence incorporates only 13 of the 32 possible states, *i.e.* o is not ergodic, as many states are never visited. Similarly, only 22 rules of the 256-rules ECA rule space drive the 42-step t'_r sequence, so the o system is not ergodic within the ECA rule space either.)

The study of these composite ECA systems [1] satisfied the authors' objective of establishing universal requirements for OEE, but the authors recognized that their conclusions should also be relevant to the richer dynamics of large systems of mutually-interacting subsystems. I have considered two-dimensional *hodge podge machines* as a family of abstract systems of interest for studying OEE at larger spatial and complexity scales.

A two-dimensional non-linear dynamic system: the hodge podge machine

The hodge podge machine CA was an outcome of work done by Martin Gerhardt and Heike Schuster studying the phenomenon of spatially-ordered structures emerging in chemical systems [4]. Rigorous interest in the phenomenon of spontaneous oscillations in chemical media began with the Russian chemist Boris Belousov who noticed these phenomena *circa* 1950, but at first these striking observations were assumed impossible by editors and mostly ignored until Anatoly Zhabotinsky later expanded on the work and developed credible theory. Since recognition of the Belousov-Zhabotinsky (BZ) reaction [2], other oscillating nonlinear chemical systems have been discovered and studied.

Reference [3] is an article about the hodge podge (HP) machine for a general readership. Note that there is scope for some variation in parameter values and in the state-transition rules, so a continuous universe of varied hodge podge machines can be defined.

Methods

For the purposes of this work, my modification of the HP machine as described in [3] incorporates a much-reduced number of states (n = 7, specifying cell-state set 0 to 7), horizontal and vertical periodic boundary conditions (toroidal topology), and seven-cell neighbourhoods (Figure 2, below) implemented on a CA grid of 300 x 300 cells. In all implementations, the grid was initialized with a uniform (pseudo) random distribution of the cell states.

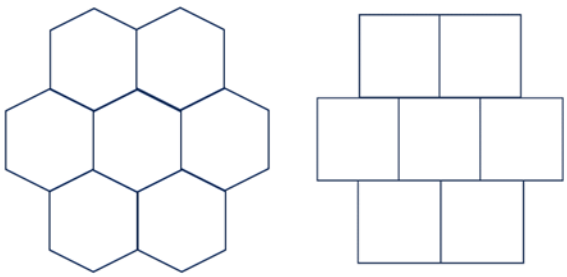

Figure 2 (above). A seven-cell CA neighbourhood is described elegantly with hexagonal cells (**left**), but can be implemented more simply in a CA grid of square cells with rows staggered by a half-cell distance in an alternating manner (**right**). In a CA grid of seven-cell neighbourhoods, an even number of equal-length rows allows periodic boundary conditions to be applied both vertically and horizontally. With each cell implemented as 2x2 pixels, the half-cell displacements of neighbouring rows correspond to horizontal shifts of one pixel.

The hodge podge machine rules implemented in this work

The eight states can be categorized as 0 ("healthy"), 1 to 6 (progressively "infected"), and 7 ("ill"). All **ill cells** (state 7 at time t) transition to healthy cells (state 0) at time t+1.

Healthy cells (state 0 at time t) transition to a state at time t+1 calculated by:

floor(number of not-ill cells over the 7-cell neighbourhood / k1) + floor(number of ill neighbour cells / k2)

Infected cells (in the state range 1 to 6 at time t) transition to a state at time t+1 calculated by:

floor(((sum of state values over the 7-cell neighbourhood) / (number of neighbouring not-ill cells)) + g)

The calculated state is truncated to state 7 if the calculation result exceeds 7. If the number of neighbouring not-ill cells denominator evaluates to zero, value 1 corresponding to the infected neighbourhood centre cell is substituted which avoids a **DIV by 0** condition. The g parameter term is a contribution which influences "infectivity".

By the further modifications of setting parameters k1 to 2/1.1, k2 to 3/1.6, and g to 0.42, visually-satisfying classic BZ dynamics of spirals and scrolls are produced by my HP machine implementations, as shown in the screenshot stills of Figure 3A below. Casual comparison of the two frames of Figure 3A indicates a system period of nine time-steps, but close inspection reveals that the frames differ very slightly, *i.e.* the system has converged to a short-period cycle, but not exactly - the cycle drifts slowly within the system's state-space, but in time eventually completes convergence to an exact short cycle. As an aside, Figure 3B relates hodge podge machine dynamics to the observable dynamics of a fertilized starfish egg surface, contributing to an argument for the relevance of hodge podge machines to general biological dynamics.

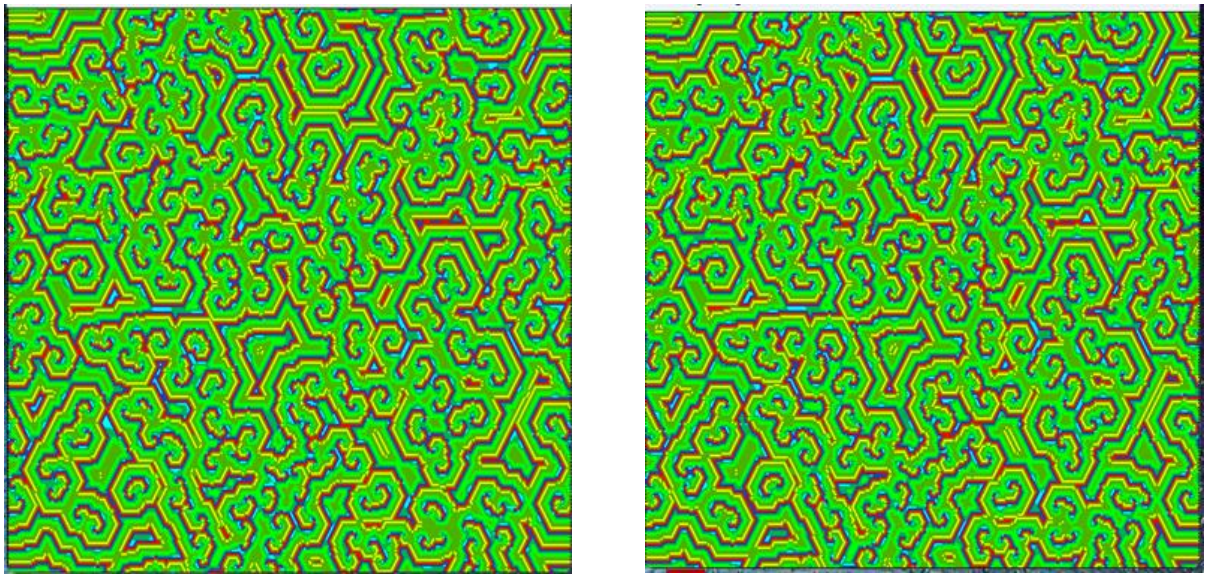

Figure 3A. Screenshot stills of a hodge podge machine implementation illustrating a short, but not yet exact, state cycle (see discussion in the text). **Left**, At time 214. **Right**, At time 223 (time interval 9 steps). Parameter values: k1 = 2/1.1, k2 = 3/1.6, g = 0.42, and n = 7 (state set 0 to 7). Cell states 0 to 7 are represented with the colour assignments shown in Figure 4.

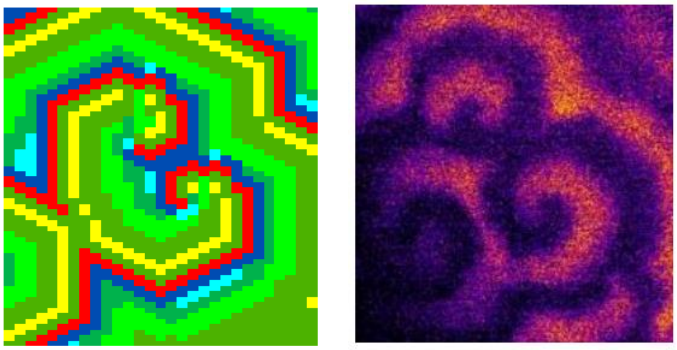

Figure 3B. Left: A Zhabotinsky scroll isolated from a separate run of the hodge podge machine shown in Figure 3A. **Right:** A strikingly-similar image of the surface of a newly-fertilized starfish egg, cropped from a larger micrograph by Jörn Dunkel, Nikta Fakhri *et al.*, shown in a 2020 MIT news release at https://news.mit.edu/2020/growth-organism-waves-0323 (This online news release includes video of the dynamically-changing egg surface.)

Figure 4. In all of my CA graphics, cell states are visualized by colour. State 0 (healthy) through infected (states 1 to 6) to state 7 (ill) are represented respectively by the left-to-right colour sequence from red to deep blue.

With varied combinations of parameter values, a continuous range of different hodge podge machines can be constructed. Varying the g parameter value with all else held unchanged corresponds to a satisfying degree of dynamic variability, which can be seen in comparison of the graphics shown in Figure 5 and Figure 3A. Figure 5 below shows an implementation differing from

that shown in Figure 3A only by changing the g parameter value from 0.42 to 0.80. With only this change, different dynamics are readily apparent. (Figure 5 spans the next three pages, with commentary following.)

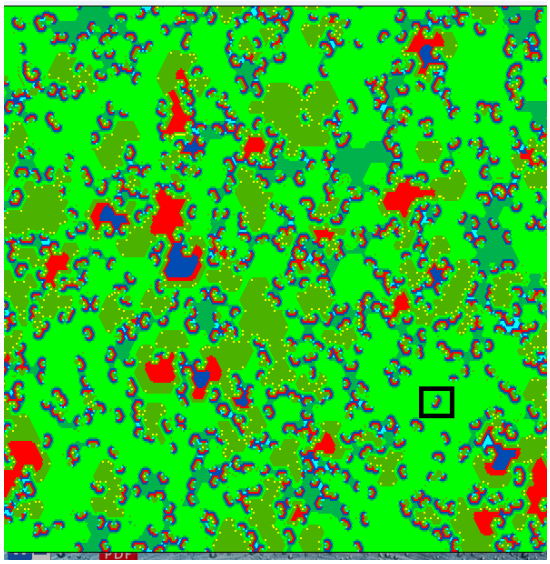

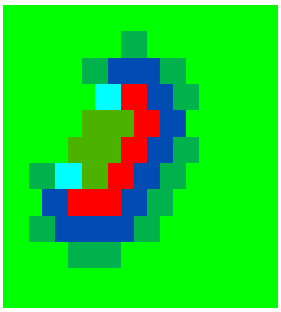

Time 130

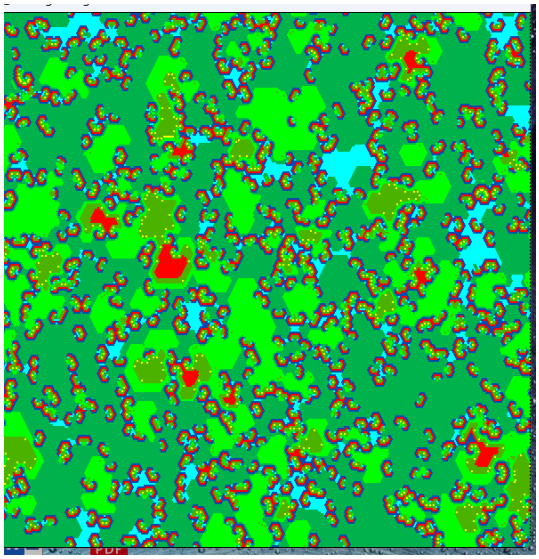

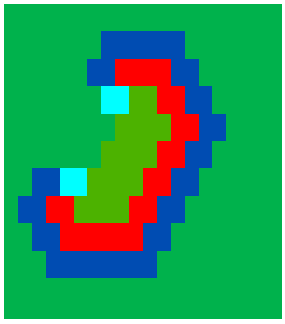

Time 131

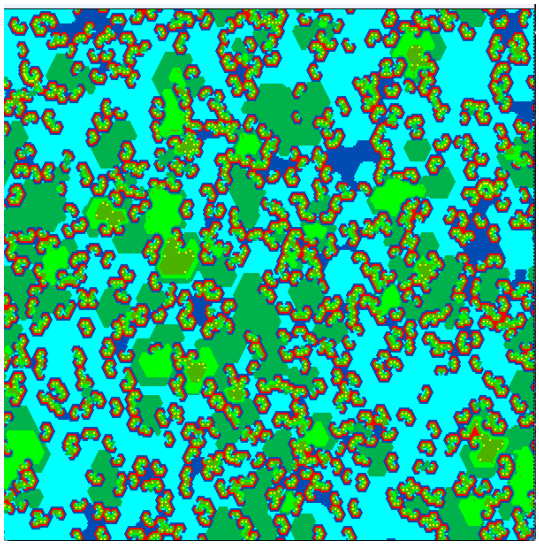

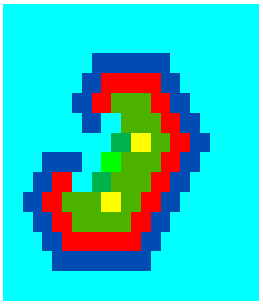

Time 132

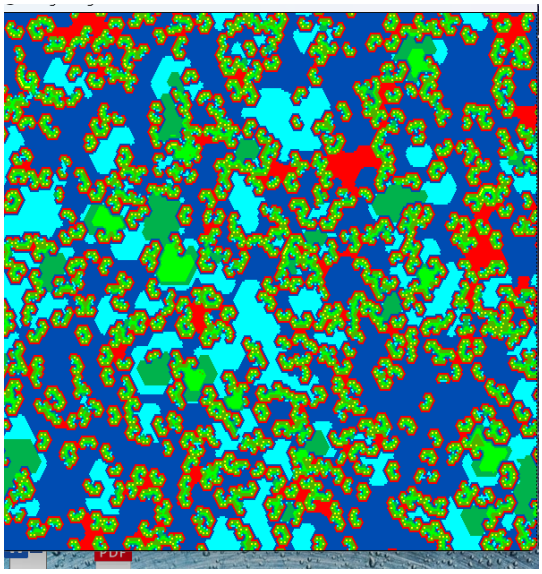

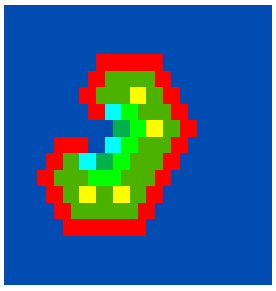

Time 133

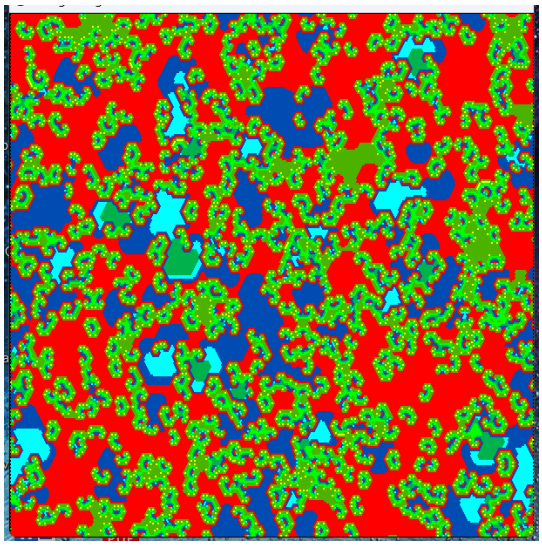

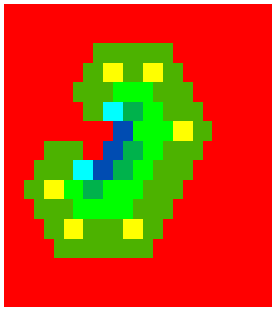

Time 134

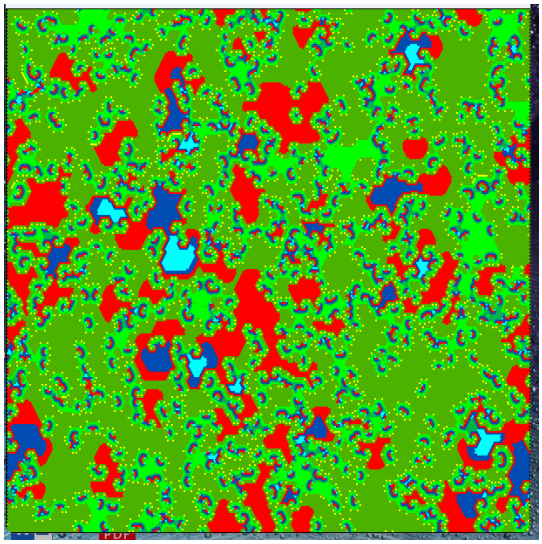

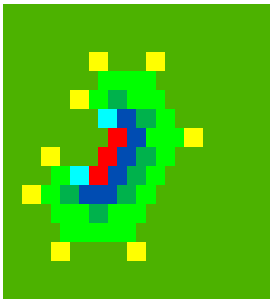

Time 135

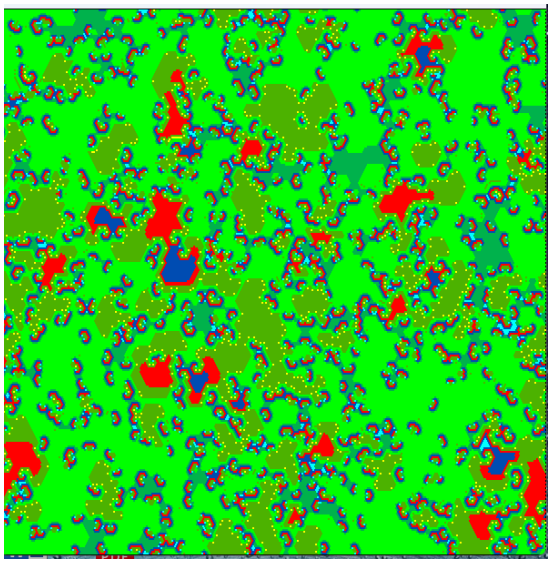

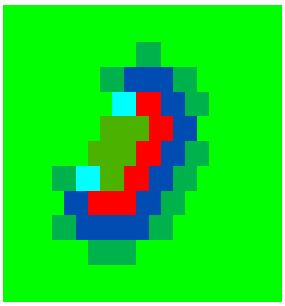

Time 136 (same as Time 130, closing the cycle)

Figure 5. Screenshot stills of a hodge podge machine implementation demonstrating an exact six-step cycle (see discussion in the text). Parameter values: k1 = 2/1.1, k2 = 3/1.6, g = 0.80, and n = 7 (state set 0 to 7).

With g = 0.80, the six-step cycle (time = 130 to 136) shown in Figure 5 above displays dynamics very different from the dynamics illustrated in Figure 3A where g = 0.42 (all else equal). An immediately-noticeable feature in Figure 5 is the structural contrast between a scattering of small detailed structures and the background mosaic of larger patches of cells of uniform state-value. At time = 130, one of the small structures isolated within a patch of cells in state 4 (bright green) is selected and identified within a rectangular black border. Zoom-views of this structure are shown to the right of the corresponding full grid at each time step, showing its cyclic dynamic within the six-step cycle.

Interaction of three hodge podge machines

Recognizing that OEE can emerge in a composite system of one subsystem perturbed by another, I have explored systems of mutually-interacting two-dimensional HP machines differing only in the

values of the g parameter. Figure 6 details how I have organized the mutual interaction of three two-dimensional HP machines, distinguished by g values 0.42 and 0.80 as in Figures 3A and 5 respectively, and g = 0.75. In the three-layer mutual-interaction system, the HP machine rules specified on page 4 are extended from seven-cell neighbourhoods to nine-cell neighbourhoods.

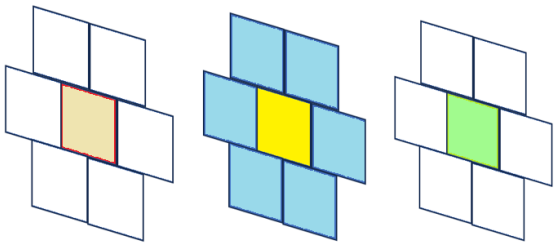

Figure 6. A seven-cell neighbourhood in each of three parallel 2D hodge podge machines. The central yellow cell with six blue neighbours is a complete neighbourhood within one HP machine evolving independently of any others. Influence from parallel HP machines was enabled by adding to the neighbourhood a cell at the same planar coordinates as the yellow cell (beige and green) in each of the other HP machines. This defines nine-cell neighbourhoods within the system of three interacting HP machines. A nine-cell neighbourhood is so-defined for every cell in the system by a periodic boundary condition applying to the dimension perpendicular to the three planes.

Results

Figure 7 below shows a time series from the g = 0.80 layer within the three mutually-interacting layers system. The first image occurred at Time = 209 with subsequent images at successive six-step intervals. Fifty time-steps of mutual independence of the HP machines were allowed before mutual interactions were enabled (*i.e.* one additional neighbour from each of the other layers added to each neighbourhood from Time = 51). In all three layers k1 = 2.0/1.1 and k2 = 3.0/1.6.

While the independent HP machine with g = 0.80 settles into a strict six-step cycle (Figure 5), Figure 7 below shows that the six-step cycle drifts in response to the additional inputs from the other layers in the mutually-interactive system. This demonstrates that in the three-layer system, t_r of the g = 0.80 layer extends to a period much longer than six steps. See **Discussion** for commentary on this point.

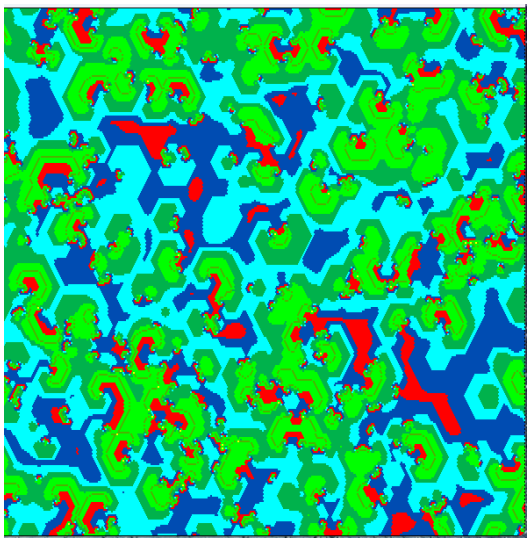

Time = 209

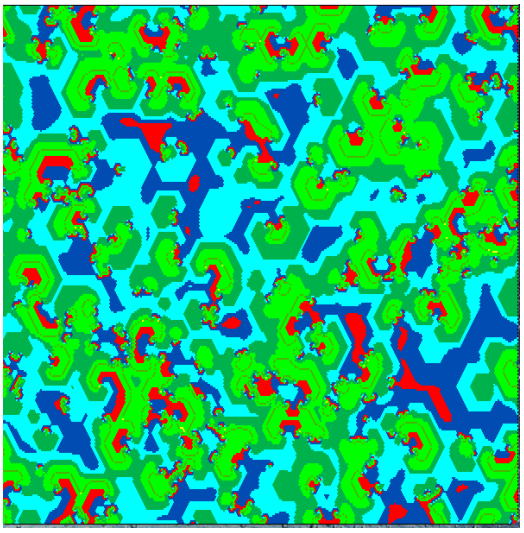

Time = 215

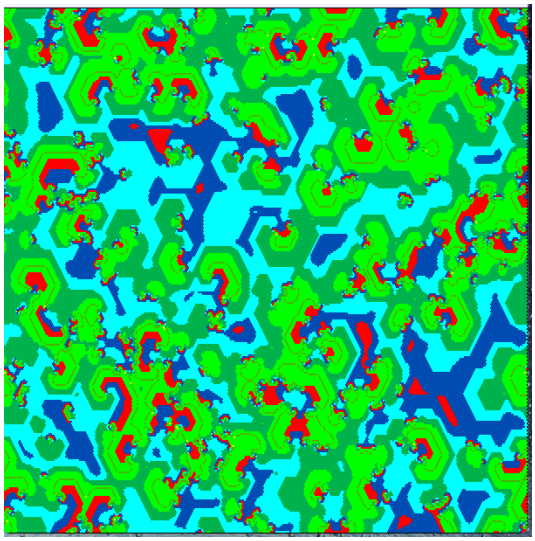

Time = 221

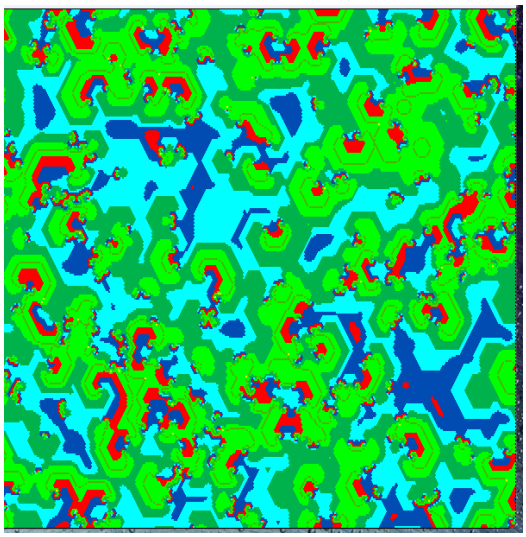

Time = 227

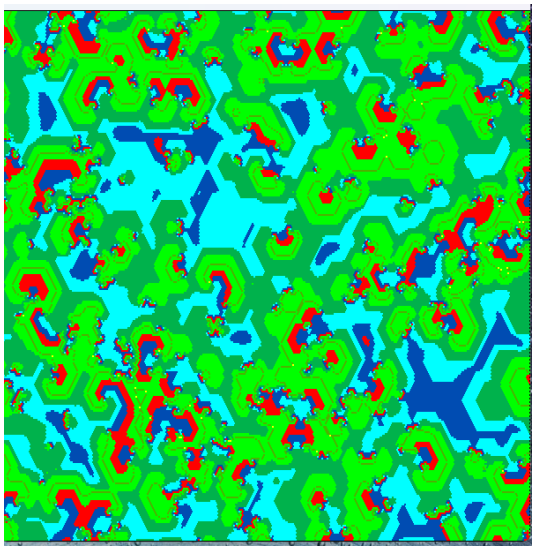

Time = 233

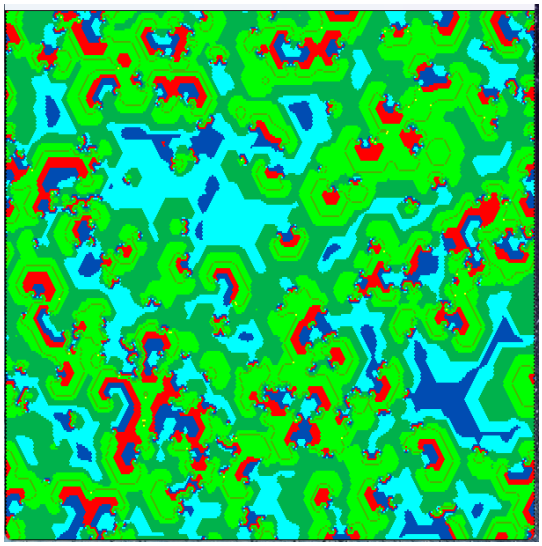

Time = 239

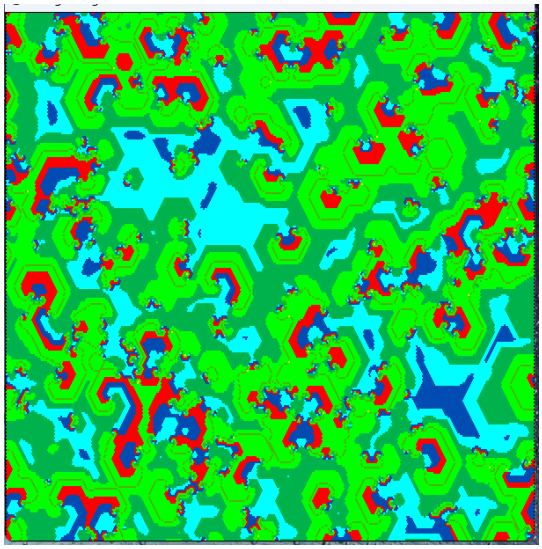

Time = 245

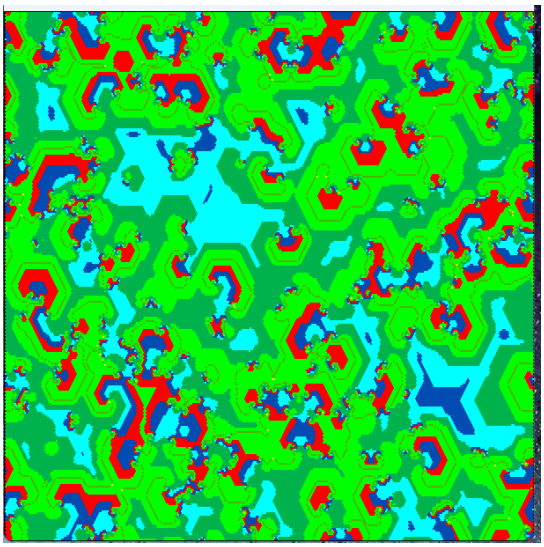

Time = 251

Figure 7. A time series of the g = 0.80 subsystem layer within the three-layer mutually-interacting system. The first image (top left) occurred at Time = 209 with subsequent images at successive six-step intervals, the last (8th, bottom right) being at Time = 251. Fifty time-steps of mutual independence were allowed before the mutual interaction was switched on (*i.e.* one additional neighbour from each of the other layers were added to each neighbourhood from Time = 51). In all layers, the k parameter values were set to k1 = 2.0/1.1 and k2 = 3.0/1.6 (the layers differed only in the value of the g parameter).

Time series sequences are not shown for the layers determined by g values 0.75 and 0.42, but Figure 8 below shows screenshot stills of these layers at Time = 251, for comparison with the Time = 251 screenshot shown in Figure 7. Visual comparisons indicate that the comprehensive system of three interacting HP machine layers eventually converges to a homogeneous dynamic very different from the dynamics of the individual HP machines iterated in isolation from each other.

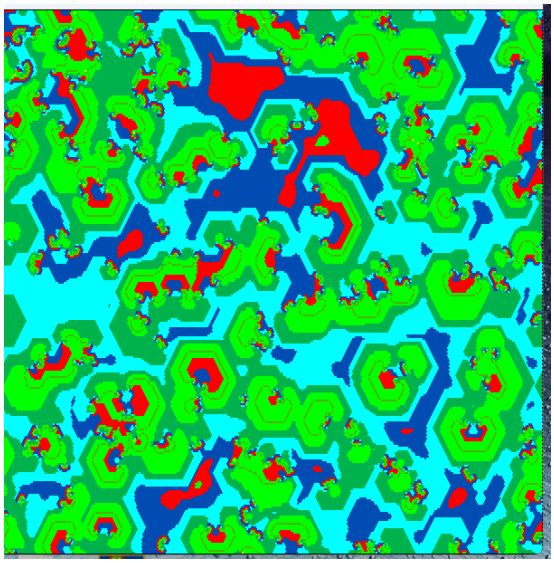

g = 0.75, Time = 251

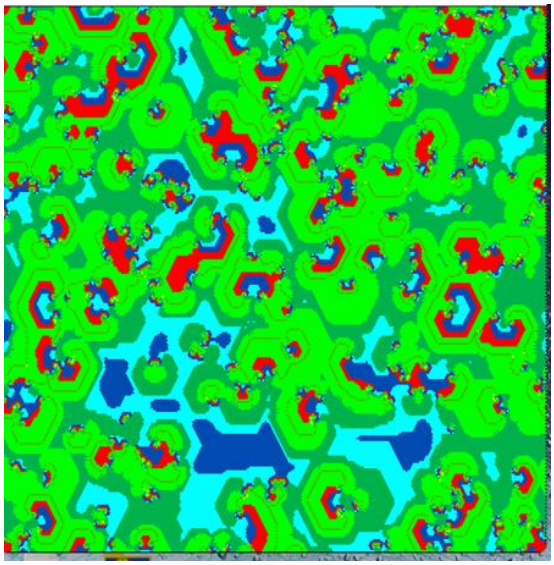

g = 0.42, Time = 251

Figure 8 (above). Representative screenshots of subsystem layers with g = 0.75, **left**, and with g = 0.42, **right**, at Time = 251. All three mutually-interacting layers appear to converge to a similar dynamic (in particular, the g = 0.42 layer loses its characteristic BZ spirals-and-scrolls structure displayed in Figure 3A).

The innovation (INN) definition can be satisfied by identification of rule contradictions

Within a system of interacting subsystems, innovation can be recognized where the state trajectory of a subsystem cannot occur in an equivalent independent system [1]. Observation of arbitrarily-selected neighbourhoods in the system of three mutually-interacting HP machines revealed instances of state-transition contradictions within their HP machine layers. A seven-cell neighbourhood within its specific subsystem layer is part of a corresponding nine-cell neighbourhood within the system of interacting layers (see Figure 6), so the within-layer state-transition contradictions are readily explained by variation of the states of the two additional cells completing the nine-cell neighbourhood. There is no single independent HP machine which can accommodate different cell state transitions at different times from a common neighbourhood state, so observation of these within-layer contradictions satisfies the definition of INN given in [1].

Tables 1 to 3 below show instances of within-layer state-transition contradictions. Colour-highlighting corresponds to the colour-coding shown in Figure 6, so the geometry of these results can be visualized. (Note that common centre state neighbourhoods are state-transition-context identical if the distribution of states within the neighbourhoods is invariant, *e.g.* the third pair of seven-cell neighbourhoods listed in Table 1 are 4 (centre), 3, 4, 4, 3, 4, 4 and 4 (centre), 4, 4, 4, 4, 3, 3. These are identical seven-cell neighbourhoods in differing nine-cell neighbourhoods.)

Table 1. Cell state transitions recorded from observations of an arbitrary seven-cell neighbourhood colour-coded yellow (centre, C) and blue (its neighbours) within a subsystem layer with g = 0.80. The nine-cell neighbourhood in the mutually-interacting system is completed by one cell from each of the parallel HP machine layers (colour-highlighted beige and green). The g parameter values set for the parallel layers were 0.42 and 0.75. Each of the three row-pairs demonstrate a within-layer state transition contradiction.

Time	C, state at the centre of the neighbourhood	States of the six neighbours of C in the 7-cell neighbourhood within the g = 0.80 HP layer						States of additional neighbours in parallel HP machine layers		State transition C --> * in the system of three mutually-interacting layers	Comments
65	6	6	5	6	5	6	6	4	5	6	maintenance of infection
84	6	6	5	6	5	6	6	4	6	7	infected --> ill
127	4	4	4	4	4	4	4	4	4	5	infection increase
132	4	4	4	4	4	4	4	0	4	4	maintenance of infection
113	4	3	4	4	3	4	4	4	4	5	infection increase
126	4	4	4	4	4	3	3	0	4	4	maintenance of infection

Table 2. Cell state transitions recorded from observations of an arbitrary seven-cell neighbourhood colour-coded yellow (centre, C) and blue (its neighbours) within a subsystem layer with g = 0.42. The nine-cell neighbourhood in the mutually-interacting system is completed by one cell from each of the parallel HP machine layers (colour-highlighted beige and green). The g parameter values set for the parallel layers were 0.80 and 0.75. Each of the three row-pairs demonstrate a within-layer state transition contradiction.

Time	C, state at the centre of the neighbourhood	States of the six neighbours of C in the 7-cell neighbourhood within the g = 0.42 HP layer						States of additional neighbours in parallel HP machine layers		State transition C --> * in the system of three mutually-interacting layers	Comments
352	5	6	6	5	6	5	5	6	6	6	increase in infection
489	5	6	6	5	6	5	5	7	7	7	increase in infection
64	4	4	4	4	4	4	4	5	5	5	increase in infection
69	4	4	4	4	4	4	4	4	4	4	maintenance of infection
137	4	4	4	4	3	4	4	4	4	4	maintenance of infection
150	4	4	4	4	4	3	4	5	5	5	increase in infection

Table 3. Cell state transitions recorded from observations of an arbitrary seven-cell neighbourhood colour-coded yellow (centre, C) and blue (its neighbours) within a subsystem layer with g = 0.75. The nine-cell neighbourhood in the mutually-interacting system is completed by one cell from each of the parallel HP machine layers (colour-highlighted beige and green). The g parameter values set for the parallel layers were 0.80 and 0.42. Each of the six row-pairs demonstrate a within-layer state transition contradiction.

Time	C, state at the centre of the neighbourhood	States of the six neighbours of C in the 7-cell neighbourhood within the g = 0.75 HP layer						States of additional neighbours in parallel HP machine layers		State transition C --> * in the system of three mutually-interacting layers	Comments
91	5	5	5	5	6	6	5	7	5	7	infected to ill
179	5	5	6	5	6	5	5	5	4	6	infection increase
266	5	4	5	4	5	5	5	5	3	5	infection maintained
322	5	4	5	4	5	5	5	5	4	6	infection increase
247	4	4	4	4	4	4	4	4	4	5	infection increase
252	4	4	4	4	4	4	4	4	0	4	infection maintained
240	4	4	4	4	3	4	4	4	0	4	infection maintained
259	4	4	4	3	4	4	4	4	4	5	infection increase
190	4	3	4	4	4	3	4	4	4	5	infection increase
196	4	4	3	4	4	3	4	4	0	4	infection maintained
74	4	0	0	0	0	4	4	5	7	4	infection maintained
94	4	0	0	0	4	0	4	4	0	2	infection decreased

Discussion

The example from [1] reproduced above in Figure 1 demonstrates OEE in a system with state-dependent dynamics, *i.e.* each state transition of the “organism” (o) subsystem is a function of its preceding ECA state-transition rule, but at each step the rule is perturbed by the state of the “environment” (e) subsystem.

Like the class 1 ECA systems studied in [1], the time-course of each HP machine layer in the system of three interacting layers is determined by both within-layer cell-states and cell-states of the adjoining HP machine layers (the nine-cell neighbourhoods span all layers, Figure 6). But unlike the class 1 ECA systems, each HP machine layer (each subsystem) perturbed by the dynamics of its neighbouring subsystems simultaneously perturbs the dynamics of the neighbouring layers. Another contrast with the class 1 ECA systems studied in [1] is that in the HP machine systems, the nine-cell neighbourhood state transition rules applied across the three-layer system are *static in time*, but in the restricted scope of each single HP machine layer, the component seven-cell neighbourhoods within their respective nine-cell neighbourhoods often correspond to contradictory cell state transitions (Tables 1 to 3).

Despite these differences, both classes of systems can satisfy the INN feature of subsystem histories which have no isolated-system equivalents, but the increased size and complexity of the three interacting HP machines system deliberately addresses the problem of identifying OEE in real-world systems of interest. Considering the unbounded evolution (UE) aspect of OEE, a 300 x 300 cell HP machine layer with an 8-member cell-state set has $t_p = 8 \text{ ^ } (300 \times 300) > 10\text{^}81{,}278$. This vast number excludes recognition of any $t_r > t_p$ identifying UE of a subsystem (see **Footnote** below), so the potentially tractable approach to assessment of OEE in large, complex systems is hypothetically restricted to assessment of INN, which was shown to scale with recurrence time over the range of systems studied in [1].

It is encouraging that identification of some state transition contradictions within a layer due to perturbation from parallel interacting layers is easily tractable (Tables 1 to 3), but a question to address is: how extensive must a compilation of state transition contradictions be to reliably identify robust OEE of a subsystem?

Noting that biology is homochiral (defined by right-handed nucleic acids and the left-handed proteins determined by transcription and translation), what are the prospects for development of a general dynamic system applicable to both biological and artificial systems that is both homochiral and open-ended? Some immediate observations may be relevant. A Zhabotinsky scroll (Figure 3B) consists of two joined spirals. One spirals inward in the clockwise direction, and its complement partner spirals inward in the counter-clockwise direction, so in a sense a HP machine displaying classic BZ dynamics (*e.g.* Figures 3A and 3B) is a racemic conglomeration of chiral dynamic components. At a spatial scale localized sufficiently to limit observation of only single spirals, an impression of homochirality might be perceived. Is there any relevance here for reconciliation of homochiral dynamics (*e.g.* as observed in study of CA loop replicators) with dynamic systems driven by achiral rules (*e.g.* Game of Life and HP machines)? Recognition of the strengths and limitations of each class of systems may inspire some unification of the two to form life-like open-ended homochiral systems, perhaps further inspiring a credible solution to the abiogenesis problem.

Footnote: While the extension of t_r resulting from perturbation of the g = 0.08 subsystem (Figure 7) may be encouraging for prospective recognition of UE ($t_r > t_p$), the vast value of t_p excludes confirmation of UE of the subsystem.

Acknowledgement

All of my CA graphics were generated from scripts written and run using *Processing* software [5].

References

[1] A Adams, H Zenil, PCW Davies and SI Walker, Formal Definitions of Unbounded Evolution and Innovation Reveal Universal Mechanisms for Open-Ended Evolution in Dynamical Systems, *Scientific Reports* **7**(1):997 (2017).

[2] BP Belousov, A periodic reaction and its mechanism, **In** RJ Field and M Burger (editors), *Oscillations and traveling waves in chemical systems*, Wiley, New York (1985).

[3] AK Dewdney, Computer Recreations. The hodgepodge machine makes waves, *Scientific American* (August 1988) 86-89.

[4] M Gerhardt and H Schuster, A cellular automaton describing the formation of spatially ordered structures in chemical systems, *Physica D* **36** (1989) 209-221.

[5] C Reas and B Fry, *Processing, A Programming Handbook for Visual Designers and Artists* (second edition). MIT Press, Cambridge MA (2014).

[6] S Wolfram, *A New Kind of Science.* Wolfram Media, Inc., Champaign IL (2002).